Polyhedron 173 (2019) 114142

Contents lists available at ScienceDirect

Polyhedron

journal homepage: www.elsevier.com/locate/poly

Synthesis and characterization of butylamine-functionalized Cr(III)–MOF–SO_3H: Synergistic effect of the hydrophobic moiety on Cr(III)–MOF–SO_3H in esterification reactions

Masoumeh Karimi Alavijeh, Mostafa M. Amini *

Department of Chemistry, Shahid Beheshti University, G.C., Tehran 1983963113, Iran

ARTICLE INFO

Article history:
Received 23 June 2019
Accepted 1 September 2019
Available online 10 September 2019

Keywords:
MIL-101(Cr)–SO_3H
Synergistic effect
Hydrophobic group
Esterification
Solvent-free condition

ABSTRACT

Mesoporous solid acid catalysts with partially hydrophobic moieties, $[Cr_3O(BDC–SO_3H)_{3-x}(BDC–SO_3NH_3Bu)_x]_n$, were prepared from $[Cr_3O(BDC–SO_3H)_3]_n$ (MIL-101(Cr)–SO_3H) and $BuNH_2$ for the first time and then characterized by the Brunauer–Emmet–Teller (BET) technique, powder X-ray diffraction, field emission electron microscopy, Fourier transform infrared spectroscopy, and thermal and elemental analyses. The nitrogen adsorption–desorption study showed that the specific surface area and total pore volume of MIL-101(Cr)–SO_3H decreased after the reaction with butylamine and formation of $[Cr_3O(BDC–SO_3H)_{3-x}(BDC–SO_3NH_3Bu)_x]_n$. The prepared materials were used as catalysts to investigate the impact of hydrophobic moieties in esterification yields of phthalic anhydride with several alcohols as a probe reaction. The presence of butylamine as a hydrophobic group on MIL-101(Cr)–SO_3H increases the esterification yield significantly for hydrophilic alcohols under solvent-free conditions. Moreover, results showed that $[Cr_3O(BDC–SO_3H)_{3-x}(BDC–SO_3NH_3Bu)_x]_n$ can be recovered and reused for several consecutive reactions without significant loss in catalyst activity.

1. Introduction

Metal–organic frameworks (MOFs) are porous coordination networks composed of a combination of metal ions and organic ligands. Due to their unique properties, including high surface area, easy adjustment of cavity size, and functionalized structure tailored to the type of need [1–3], MOFs have become one of the leading nanostructured materials for a variety of fields such as adsorption [4], gas storage and separation [5,6], drug delivery [7], sensor [8], and heterogeneous catalysis [9–12]. MIL-101(Cr) among the reported MOFs due to its large pore volume, high surface area, and high thermal and chemical stability has been employed extensively as a catalyst in the chemical reactions in comparison to other MOFs under catalytic circumstances.

Esterification reaction is one of the potential applications of MOF solid acids [13], but the hydrophilic nature of most MOFs prevents a high yield of esterification reactions. The presence of water in the esterification reaction as an inevitable byproduct can significantly affect the reaction efficiency. Hence, the development of heterogeneous catalysts with large and well-ordered pores to minimize diffusion restrictions, acidic sites for catalysis reaction and hydrophobic surfaces to overcome water effects is necessary. For various applications, a number of studies have been focused on different strategies to increase the hydrophobicity and stability of the solid catalysts [14,15], including MOFs [16,17], by introducing different hydrophobic moieties.

In the esterification reactions, the use of acid catalysts [18,19] has grown more than neutral [20–24] and alkaline catalysts [25–33]. Among the acid catalysts used in esterification and transesterification for the production of a wide variety of esters and biofuel, sulfuric acid [34], titanate [35,36], ionic liquids [37–42], and many solid acids [43–47] can be mentioned. However, most of these catalysts have several drawbacks, such as high cost, deactivation, prolonged reaction time, water adsorption by the catalyst, isolation problems, low stability, and low levels of acid sites. More importantly, an esterification reaction is an equilibrium process in which water is produced as a byproduct, and reaction reach a plateau in low yield. The Dean–Stark trap is used to solve this problem, but this system cannot be used for light and hydrophilic alcohols. In addition, the esterification efficiency of acidic alcohols, such as fluorinated alcohols, is particularly low, which makes the production of their esters expensive. Therefore, the introduction of acidic catalysts that simultaneously have hydrophobic properties seems to be a logical solution to overcome this problem. In this context, introducing catalysts without the issues mentioned above appears

---

* Corresponding author. Fax: +98 21 22431663.
E-mail address: m-pouramini@sbu.ac.ir (M.M. Amini).

https://doi.org/10.1016/j.poly.2019.114142
0277-5387/

to be necessary. Therefore, MOF solid acids containing hydrophobic moieties are targeted herein as heterogeneous catalysts for the transformation of phthalic anhydride into a related ester.

In this study, our objective was to introduce a dual-functionalized MIL-101(Cr) with $–SO_3H$ and hydrophobic moieties, for the first time as a potent solid acid catalyst to improve yields of esterification reactions by the repulsion of the produced water from the reaction cage, and also to be able to recover and reuse catalyst. Concomitantly, the impact of surface hydrophobicity of the catalyst on the esterification yield of phthalic anhydride as a probe reaction was investigated. In addition, to examine the effect of alcohol type on the reaction yield in the presence and absence of hydrophobic moieties, several alcohols were used for esterification, and also a new ester of phthalic anhydride was introduced.

2. Experimental

2.1. Materials and instrumentation

All chemicals and solvents were purchased from Merck Chemical Company (Darmstadt, Germany), Sigma-Aldrich Chemical Company (Dorset, UK), TCI Chemicals and used without purification. Merck precoated silica-gel 60 F254 plates were used to perform thin-layer chromatography (TLC), and compounds were visualized with 254 nm ultraviolet light. Column chromatography was carried out on silica gel 60 (0.063–0.200 mm). Infrared spectra were recorded on a Bomem MB-Series FTIR spectrometer. ^1H, ^{13}C, and ^{19}F NMR data were collected on a Bruker AVANCE 300 MHz spectrometer utilizing $CDCl_3$ as solvent and tetramethylsilane as internal standard. Mass spectrometry was performed with an Agilent 5975C VL MSD (ion source: EI, 70 eV). A STOE diffractometer equipped with Cu Kα radiation ($\lambda = 0.15418$ nm) was used to record powder X-ray diffraction (XRD) patterns. Thermogravimetric analysis (TGA) was performed using a Bahr STA-503 instrument at a heating rate of 10 °C min^{-1} under a flow of air. The SEM micrographs were taken using a field emission scanning electron microscope (MIRA3 TESCAN). Surface area and texture properties of the prepared catalyst were determined by N_2 physisorption technique on a Belsorp-miniII porosimeter. The CHN elemental analysis was accomplished using a Perkin-Elmer 2400 CHN analyzer.

2.2. Preparation of MIL-101(Cr) and MIL-101(Cr)–SO_3H ($[Cr_3O(BDC–SO_3H)_3]_n$)

To a well grinded mixture of $Cr(NO_3)_3·9H_2O$ (2.0 g, 5 mmol) and 1,4-benzenedicarboxylic acid (BDC) (0.83 g, 5 mmol), 20 mL of water was added, and the resulting mixture was sonicated for several minutes. Subsequently, the suspension was transferred to a Teflon-lined stainless-steel autoclave, and the autoclave was heated at 220 °C in an oven for 24 h. After cooling the autoclave to ambient temperature, MOF-101(Cr) was isolated by centrifugation, washed with methanol and acetone, and then was immersed in DMF overnight at 70 °C. The product was then rewashed with methanol and acetone and dried at 75 °C [48]. Synthesis and purity of MIL-101(Cr) were confirmed by FTIR spectroscopy and powder X-ray diffraction. MIL-101(Cr)–SO_3H, was prepared according to the reported procedure, with some modifications [49]. For this purpose, a mixture of CrO_3 (1.25 g, 12.50 mmol), monosodium 2-sulfoterephthalic acid (3.35 g, 12.50 mmol), and 12 M hydrochloric acid (0.91 g, 25 mmol) was dissolved into 50 mL of deionized water and stirred for a few minutes at ambient temperature. The resulting mixture was then transferred to a Teflon-lined stainless-steel autoclave, and the autoclave was heated in an oven at 180 °C for six days. After separating the green solid product by centrifugation, it was washed three times with distilled water and methanol. The product was dried at 50 °C overnight. Anal. Calc. (Found) for $[Cr_3O(BDC–SO_3H)_3]_n·25H_2O$: C, 20.47 (19.80); H, 4.80 (4.40). The acidity of MIL-101(Cr)–SO_3H was measured according to the earlier report [49]. In a typical procedure, 0.50 g of MIL-101(Cr)–SO_3H was immersed in a saturated aqueous solution of NaCl and stirred at room temperature for 12 h. Subsequently, the filtrate was titrated with a 0.1 M NaOH solution.

2.3. Preparation of $[Cr_3O(BDC–SO_3H)_{3-x}(BDC–SO_3NH_3Bu)_x]_n$

For the synthesis of $[Cr_3O(BDC–SO_3H)_{3-x}(BDC–SO_3NH_3Bu)_x]_n$, 100 mg of MIL-101(Cr)–$SO_3H$ was placed in a Schlenk tube and evacuated for 2 h at ambient temperature. Then, the tube was flushed with dry nitrogen, and solutions containing 0.03, 0.06, and 0.09 mmol of butylamine in dry THF were added (Fig. 1). The mixture was then stirred at ambient temperature under a nitrogen atmosphere for 24 h. The product was collected by centrifugation and washed two times with 2 mL of dry THF for 15 min each time, three-times with 2 mL of dry methanol for 15 min each time, and one time for 12 h. Finally, the product was washed four times with 2 mL of deionized water for 15 min each time, and one time for 12 h, and then was dried at 50 °C overnight [50]. Anal. Calc. (Found) for $[Cr_3O(BDC–SO_3H)_{2.7}(BDC–SO_3NH_3Bu)_{0.3}]_n.14H_2O$ (10% $BuNH_2$): C, 24.57 (25.11); H, 3.95 (3.64); N, 0.34 (0.35); for $[Cr_3O(BDC–SO_3H)_{2.4}(BDC–SO_3NH_3Bu)_{0.6}]_n·11H_2O$ (20% $BuNH_2$): C, 26.43 (26.79); H, 3.83 (3.19); N, 0.70 (0.71); and for $[Cr_3O(BDC–SO_3H)_{2.1}(BDC–SO_3NH_3Bu)_{0.9}]_n·9H_2O$ (30% $BuNH_2$): C, 27.96 (27.78); H, 3.82 (3.43); N, 1.06 (0.96).

2.4. General procedure for catalytic reaction

In a typical catalytic test, 4 mmol of phthalic anhydride and 20 mmol of alcohol were loaded to a flask equipped with a condenser, and then 60 mg of MIL-101(Cr)–SO_3H or $[Cr_3O(BDC–SO_3H)_{2.4}(BDC–SO_3NH_3Bu)_{0.6}]_n$ (20% $BuNH_2$) was added as the catalyst. The reaction was refluxed for 5 h, and then the mixture was cooled to room temperature and the catalyst was separated from the reaction mass by filtration, and 100 mL of 20% aqueous solution of sodium carbonate was added. The reaction mass was extracted by CH_2Cl_2 (50 mL × 2) and the organic layer dried by sodium sulfate [34]. The crude product was purified by column chromatography using ethyl acetate/n-hexane (1:15, v:v) as an eluent, the desired compound was collected, and the yield was obtained by the weight of the product.

To evaluate the recyclability of the catalysts, the heterogeneous $[Cr_3O(BDC–SO_3H)_{2.4}(BDC–SO_3NH_3Bu)_{0.6}]_n$ (20% $BuNH_2$) was isolated by centrifugation, washed with CH_2Cl_2, dried at 50 °C, and used in a subsequent cycle.

2.5. Characterization

Di-ethyl phthalate: FTIR (KBr, cm^{-1}): 3073, 2980, 1721, 1654, 1219. ^1H NMR (300 MHz, $CDCl_3$) δ (ppm): 1.18 (t, 6H, $2(CH_3)$), 4.20 (q, 4H, $2(–OCH_2)$), 7.33 (m, 2H, 2 (Ar–H)), 7.55 (m, 2H, 2 (Ar–H)). *Di-trifluoroethyl phthalate*: FTIR (KBr, cm^{-1}): 3012, 2970, 1721, 1581, 1442, 1365, 1280, 1122, 1070, 910, 740 (Fig. S1, Supplementary Information, SI). Anal. Calc. for $C_{12}H_8F_6O_4$ (Found): C, 43.63 (43.90); H, 2.44 (2.56). MS (EI): m/z (%) = 330 (4) $[M^+]$, 316 (6), 298 (10), 279 (3), 256 (8), 239 (3), 203 (7), 185 (61), 149 (27), 112 (27), 97 (26), 83 (37), 71 (60), 57 (100), 43 (83) (Fig. S2, SI). ^1H NMR (300.00 MHz, $CDCl_3$) δ (ppm): 4.38 (q, 4H, 2 $(–OCH_2)$), 7.54 (m, 2H, 2 (Ar–H)), 7.74 (m, 2H, 2 (Ar–H)) (Fig. S3, SI). ^{13}C NMR (75.43 MHz, $CDCl_3$): 167.6 ($C{=}O$), 132.2, 130.9, 128.8 (Ar), 61.6 ($–CF_3$), 14.1 ($–CH_2$) (Fig. S4, SI). ^{19}F NMR (282.23 MHz, $CDCl_3$): -73.53 (t, 6F, $–CF_3$) (Fig. S5, SI). *Di-1-butyl phthalate*: FTIR (KBr, cm^{-1}): 3060, 2952, 2860, 1725, 1634, 1215.

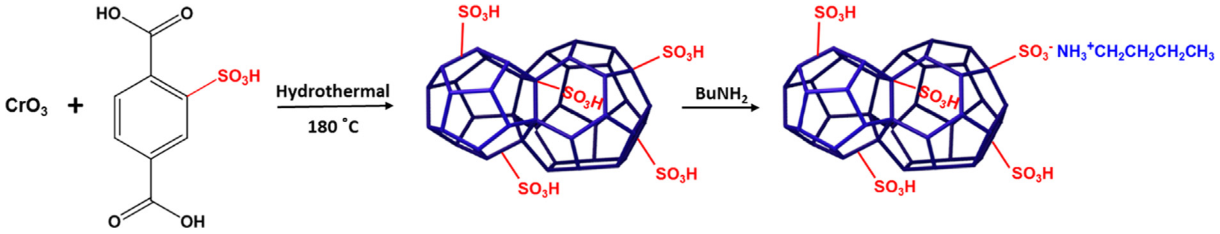

Fig. 1. Preparation of water-tolerant $[Cr_3O(BDC–SO_3H)_{3-x}(BDC–SO_3NH_3Bu)_x]_n$ for phthalic anhydride esterification.

^1H NMR (300.00 MHz, $CDCl_3$) δ (ppm): 0.92 (t, 6H, $2(CH_3)$), 1.41 (m, 4H, 2 $(–CH_2)$), 1.68 (m, 4H, 2 $(–CH_2)$), 4.27 (t, 4H, 2 $(–OCH_2)$), 7.48 (m, 2H, 2 (Ar–H)), 7.67 (m, 2H, 2 (Ar–H)). *Di-1-hexyl phthalate*: FTIR (KBr, cm^{-1}): 3062, 2930, 2858, 1726, 1603, 1286. ^1H NMR (300.00 MHz, $CDCl_3$) δ (ppm): 0.90 (t, 6H, $2(CH_3)$), 1.36 (m, 12H, 6 $(–CH_2)$), 1.73 (m, 4H, 2 $(–CH_2)$), 4.30 (t, 4H, $2(–OCH_2)$), 7.52 (m, 2H, 2 (Ar–H)), 7.72 (m, 2H, 2 (Ar–H)).

3. Results and discussion

3.1. Characterization of catalysts

MIL-101(Cr)–SO_3H was synthesized according to the earlier report using CrO_3 and monosodium 2-sulfoterephthalic acid during a hydrothermal reaction and used as an acid catalyst in the esterification of phthalic anhydride. The synthesis of MIL-101(Cr)–SO_3H was confirmed by the powder X-ray diffraction pattern. The X-ray diffraction pattern of MIL-101(Cr), MIL-101(Cr)–SO_3H, and $[Cr_3O(BDC–SO_3H)_{2.4}(BDC–SO_3NH_3Bu)_{0.6}]_n$ (20% $BuNH_2$), and the X-ray diffraction pattern of MIL-101(Cr) that simulated from the single-crystal structure, are compiled in Fig. 2. XRD patterns of the prepared materials are in accordance with the XRD pattern of MIL-101(Cr) that simulated from single-crystal structure data, and confirmed the framework structure remained intact by introducing acid groups and alkylamine on the linker of MIL-101(Cr).

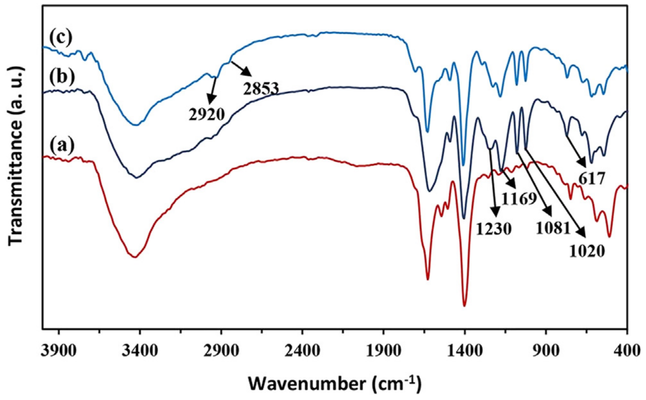

Fig. 3. FTIR spectra of the MIL-101(Cr) (a), MIL-101(Cr)–SO_3H (b), and $[Cr_3O(BDC–SO_3H)_{2.4}(BDCSO_3NH_3Bu)_{0.6}]_n$ (20% $BuNH_2$) (c).

Fig. 3 shows the FTIR spectra of MIL-101(Cr), MIL-101(Cr)–SO_3H and $[Cr_3O(BDC–SO_3H)_{2.4}(BDC–SO_3NH_3Bu)_{0.6}]_n$ (20% $BuNH_2$). The appearance of new bands at 617, 1020, 1081, 1169, and 1230 cm^{-1} in the spectrum of MIL-101(Cr)–SO_3H (Fig. 3b) in comparison with the spectrum of MIL-101(Cr) (Fig. 3a), which is associated with the stretching vibration of C—S, the stretching vibration of S—O, the in-plane skeletal vibration of the benzene ring with a sulfonic substituent, the symmetric stretching vibration mode of O═S═O, and the stretching vibration of the —SO_3H groups, respectively [51–53], shows the successful substitution of —SO_3H groups on the linker of MIL-101(Cr). Synthesis of $[Cr_3O(BDC–SO_3H)_{2.4}(BDC–SO_3NH_3Bu)_{0.6}]_n$ (20% $BuNH_2$) was confirmed by FTIR spectroscopy in addition to CHN analysis. The bands that appeared at 2920 and 2853 cm^{-1} in the spectrum of $[Cr_3O(BDC–SO_3H)_{2.4}(BDC–SO_3NH_3Bu)_{0.6}]_n$ (20% $BuNH_2$) (Fig. 3c) are associated with the aliphatic C—H group and confirmed the formation of it successfully.

Adsorption–desorption (N_2) isotherms of MIL-101(Cr)–SO_3H and $[Cr_3O(BDC–SO_3H)_{2.4}(BDC–SO_3NH_3Bu)_{0.6}]_n$ (20% $BuNH_2$) that were obtained at 77 K are shown in Fig. 4. The BET specific surface area and the total pore volume of MIL-101(Cr)–SO_3H were calcu-

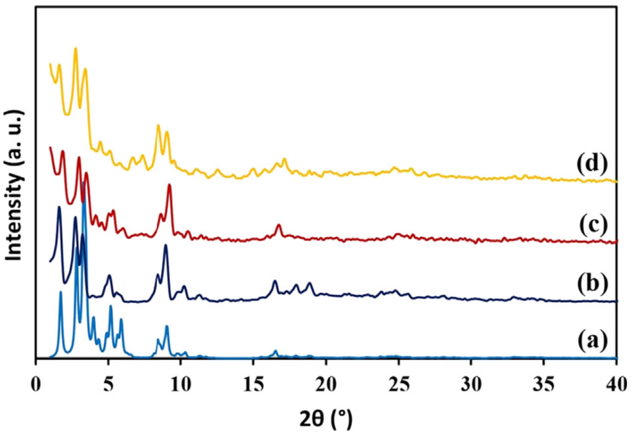

Fig. 2. Powder XRD patterns of (a) simulated MIL-101(Cr), (b) MIL-101(Cr), (c) MIL-101(Cr)–SO_3H, and (d) $[Cr_3O(BDC–SO_3H)_{2.4}(BDC–SO_3NH_3Bu)_{0.6}]_n$ (20% $BuNH_2$).

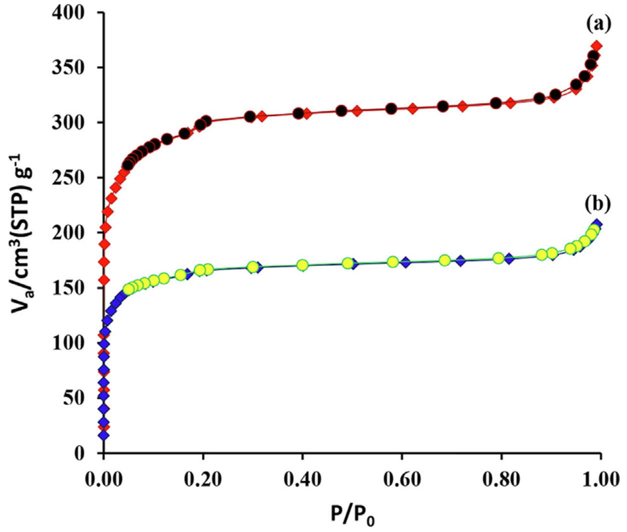

Fig. 4. N_2 adsorption–desorption isotherms of (a) MIL-101(Cr)–SO_3H, and (b) $[Cr_3O(BDCSO_3H)_{2.4}(BDCSO_3NH_3Bu)_{0.6}]_n$ (20% Bu-NH_2).

lated to be 1167 $m^2 g^{-1}$ and 0.568 $cm^3 g^{-1}$, respectively. As shown in Fig. 4, after the reaction of butylamine with MIL-101(Cr)–SO_3H and the formation of $[Cr_3O(BDC–SO_3H)_{2.4}(BDC–SO_3NH_3Bu)_{0.6}]_n$ (20% $BuNH_2$), the surface area and total pore volume of the sulfonated MIL-101 decreased to 649 $m^2 g^{-1}$ and 0.317 $cm^3 g^{-1}$, respectively [50]. This shows that the butylamines reacted to the MOF, and the resulting quaternary amines occupied some pores of MIL-101(Cr) and consequently decreased the surface area to some extent. The similarity of the adsorption–desorption profile of MIL-101(Cr)–SO_3H and $[Cr_3O(BDC–SO_3H)_{2.4}(BDC–SO_3NH_3Bu)_{0.6}]_n$ (20% $BuNH_2$) shows that although pore volume decreased from 0.568 to 0.317 $cm^3 g^{-1}$, the IV mesoporous type structure of MIL-101(Cr)–SO_3H remained intact after introducing butylamine in spite of the deformation of octahedron morphology to some extent.

To investigate the hydrophobic nature of $[Cr_3O(BDC–SO_3H)_{3-x}(BDC–SO_3NH_3Bu)_x]_n$ in comparison with MIL-101(Cr)–SO_3H, the water of both compounds was removed under vacuum at 120 °C, the compounds were exposed to water vapor, and thermogravimetric analysis (TGA) was carried out (Fig. 5). The first mass loss at about 107 °C in the thermogram of MIL-101(Cr)–SO_3H (Fig. 5a) is related to the release of water, and the second mass loss in the temperature range of about 350–475 °C is associated with the decomposition and combustion of the 2-sulfoterephthalate ligand of MIL-101(Cr)–SO_3H [54]. Notably, compared to the sulfonated MOF, $[Cr_3O(BDC–SO_3H)_{3-x}(BDC–SO_3NH_3Bu)_x]_n$ loses its water at a lower temperature (90 °C) (Fig. 5b) due to the hydrophobic nature of butylamine groups. Furthermore, a higher mass loss that occurs during decomposition and combustion of $[Cr_3O(BDC–SO_3H)_{3-x}(BDC–SO_3NH_3Bu)_x]_n$ is evidence for the presence of butylamine groups on MIL-101(Cr)–SO_3H. Thermal analysis of $[Cr_3O(BDC–SO_3H)_{3-x}(BDC–SO_3NH_3Bu)_x]_n$ is in accordance with the results of the elemental analysis that showed the containing $BuNH_2$ moiety.

Interestingly, after the water of $[Cr_3O(BDC–SO_3H)_{3-x}(BDC–SO_3NH_3Bu)_x]_n$ and MIL-101(Cr)–SO_3H was removed under vacuum and the compounds exposed to the water vapor in the same condition, according to the TGA the former showed 12 wt.% water, while the latter showed 25 wt.% water. Therefore, it can be concluded that the butyl substituted derivative of MOF is relatively hydrophobic in comparison to the one without the butyl group, which accommodated a smaller amount of water. Furthermore, to confirm the hydrophobicity of $[Cr_3O(BDC–SO_3H)_{3-x}(BDC–SO_3NH_3Bu)_x]_n$, the infrared spectrum of the samples that was used for TGA was recorded (one mg sample and 50 mg potassium bromide). As Fig. 6 shows, the IR spectrum of $[Cr_3O(BDC–SO_3H)_{3-x}(BDC–SO_3NH_3Bu)_x]_n$ did not change notably before or after being in the proximity of water; but in contrary, the intensity of the hydroxyl groups stretching band of MIL-101(Cr)–SO_3H was enhanced by 25%.

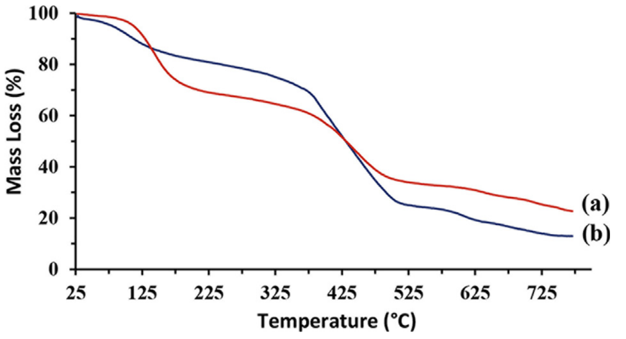

Fig. 5. Thermogravimetric analysis of (a) MIL-101(Cr)–SO_3H and (b), $[Cr_3O(BDC–SO_3H)_{3-x}(BDCSO_3NH_3Bu)x]_n$ after evacuation and exposed to water vapour for 24 h.

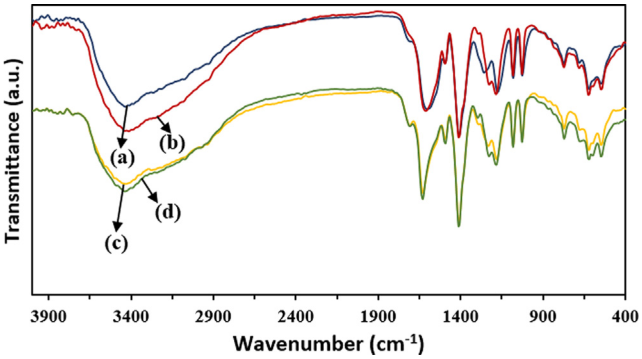

Fig. 6. Water tolerance investigation of MIL-101(Cr)–SO_3H (top) and $[Cr_3O(BDC–SO_3H)_{3-x}(BDC–SO_3NH_3Bu)_x]_n$ (bottom) by FTIR spectroscopy. Before (a and c), and after (b and d) 24 h in the vicinity of the water vapor.

The results of the FESEM analysis of MIL-101(Cr)–SO_3H showed MOF with –SO_3H retained octahedron geometry (Fig. 7a) [53], but after the anchoring of the butylamine groups, the morphology changed to a granular form to some extent (Fig. 7b).

The Bronsted acidity of $[Cr_3O(BDC–SO_3H)_3]_n$, $[Cr_3O(BDC–SO_3H)_{2.4}(BDC)_{0.6}]_n$, and $[Cr_3O(BDC–SO_3H)_{2.4}(BDC–SO_3NH_3Bu)_{0.6}]_n$ (20% $BuNH_2$) was calculated to be 1.45, 1.15, and 1.10 mmol/g by acid-base titration, respectively [53]. A drop in the number of acidic groups in the functionalized MOF in comparison with the initial MOF confirmed the presence of butylamine groups on MIL-101(Cr)–SO_3H.

3.2. Investigating the effect of various factors on the progression of phthalic anhydride esterification reaction

To study the impact of various constructing species of the catalyst on phthalic anhydride esterification, the esterification reaction was carried out in the presence of *p*-xylene-2-sulfonic acid, MIL-101(Cr), MIL-101(Cr)–SO_3H, and $[Cr_3O(BDC–SO_3H)_{3-x}(BDC–SO_3NH_3Bu)_x]_n$, and the results are illustrated in Table 1. Apparently, *p*-xylene-2-sulfonic acid, as a heterogeneous catalyst (entry 2 in Table 1) for the esterification of phthalic anhydride, showed a lower yield than MIL-101(Cr)–SO_3H (entry 4) due to the very low surface area in comparison to MIL-101(Cr)–SO_3H. Minor changes in the reaction yield in the absence of a catalyst (entry 1) to MIL-101(Cr) (entry 3) indicate that MOF Lewis acidic sites are not affected by this reaction. Also, a significant increase in the esterification yield (entry 7, 97%) with use of $[Cr_3O(BDC–SO_3H)_{2.4}(BDC–SO_3NH_3Bu)_{0.6}]_n$ (20% $BuNH_2$) as catalyst compared to $[Cr_3O(BDC–SO_3H)_{2.4}(BDC)_{0.6}]_n$ (entry 5, 55%) shows that the hydrophobic groups on the MOF play an important role in the esterification process of hydrophilic alcohols. Esterification reactions were also carried out at various times in the presence of a different amount of MIL-101(Cr)–SO_3H to find optimum reaction conditions for attaining the highest yield. The results showed that optimum time and amount of catalyst for reaching the highest yields are 5 h, and 60 mg, respectively, at reflux temperature. Notably, by increasing the mole ratio of ethanol to phthalic anhydride, the yield of reaction only increased to a small extent.

Since the formation of water in an esterification reaction slows down the process and equilibrium shifts to the starting materials, the removal of water that is generated during the process from the reaction medium is essential to advance the reaction. The use of acid catalysts that simultaneously have both acidic and hydrophobic moiety on their surface is a novel approach to overcome time-consuming and low-yield difficulties [14,15]. An acid catalyst with a hydrophobic moiety can have a synergistic effect on an esterification reaction. Such dual characteristics of a catalyst

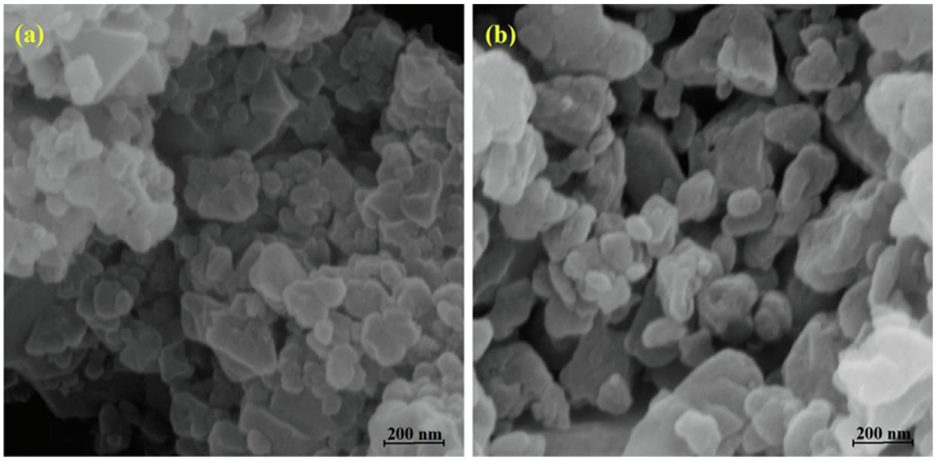

Fig. 7. The SEM images of MIL-101(Cr)–SO_3H (a), and $[Cr_3O(BDC–SO_3H)_{2.4}(BDC–SO_3NH_3Bu)_{0.6}]_n$ (20% Bu-NH_2) (b).

Table 1
The effect of hydrophobic moiety on Cr(III)–MOF–SO_3H in esterification of ethanol.

Entry	Catalyst	Yield[a] (%)
1	Blank	12.0
2	*P*-Xylene-2-sulfonic acid (Heterogeneous catalyst)	40.0
3	MIL-101(Cr)	27.5
4	$[Cr_3O(BDC–SO_3H)_3]_n$	70.0
5	$[Cr_3O(BDC–SO_3H)_{2.4}(BDC)_{0.6}]_n$	55.0
6	$Cr_3O(BDC–SO_3H)_{2.7}(BDC–SO_3NH_3Bu)_{0.3}]_n$ (10% $BuNH_2$)	80.4
7	$[Cr_3O(BDC–SO_3H)_{2.4}(BDC–SO_3NH_3Bu)_{0.6}]_n$ (20% $BuNH_2$)	97.0
8	$[Cr_3O(BDC–SO_3H)_{2.1}$ $(BDC–SO_3NH_3Bu)_{0.9}]_n$ (30% $BuNH_2$)	80.0

Reaction conditions: phthalic anhydride (4 mmol), ethanol (20 mmol), catalyst (60 mg), reaction temperature: reflux, time: 5 h.

[a] Isolated yield.

will presumably accelerate the reaction and improve the yield by acting as an acid catalyst and simultaneously discharging the generated water from the reaction cage. In this context, during a post-synthesis process, the surface of MIL-101(Cr)–SO_3H was modified with hydrophobic butylamine groups.

To confirm the role of hydrophobic groups in the esterification reaction, the esterification of phthalic anhydride with ethanol was carried out for 5 h, and then several microliters of water was added to the reaction mixture. Interestingly, the results showed that the esterification yield remained intact (97%), which indicates the repletion and tolerance of water in the process due to the presence of hydrophobic groups in $[Cr_3O(BDC–SO_3H)_{2.4}(BDC–SO_3NH_3–Bu)_{0.6}]_n$ (20% $BuNH_2$). In contrast, by the addition of several microliters of water to the same reaction mixture, with $[Cr_3O(BDC–SO_3H)_{2.4}(BDC)_{0.6}]_n$ as the catalyst without a hydrophobic group, the yield of the reaction dropped from 55% to 35%, which shows that the equilibrium shifted to the reactants due to the absence of a hydrophobic group in the catalyst.

Influences of the hydrophobic groups on the efficiency of the esterification process are demonstrated in Table 1. As shown, the effect of the hydrophobic moiety in a catalyst on the esterification of hydrophilic alcohols, such as ethanol, which adsorb a large amount of water, is noteworthy. Furthermore, there is a steady increase in the yield of esterification of ethanol by increasing the number of hydrophobic groups up to 20% (entry 7); however, in the case of further increase, the yield dropped to 80.0% (Table 1, entry 8), which is probably due to less accessibility of reactants to acidic sites as the result of steric hindrance.

To investigate the effect of alcohol type on the reaction yield, several alcohols were used in the esterification of phthalic anhydride, and also a new derivative of phthalic anhydride (entry 3 in Table 2) was reported. Esterification yields for the various alcohols are listed in Table 2. The observed trend in the yields of products in the presence of different alcohols represents a nucleophilic mechanism for the process [55]. Therefore, in the esterification of phthalic anhydride with a trifluoroethanol containing electron withdrawing substituent (entry 3), a lower efficiency was observed as expected. Apparently, two factors, steric and hydrophobic obstruction compete with each other; consequently, in esterification of long-chain alcohol (entry 7), spatial inhibition decreases the reaction efficiency.

The catalytic performance of MIL-101(Cr)–SO_3H and $[Cr_3O(BDC–SO_3H)_{2.4}(BDC–SO_3NH_3Bu)_{0.6}]_n$ (20% $BuNH_2$) as solid acid catalysts in the esterification of phthalic anhydride with ethanol is compared with several other homogeneous and heterogeneous catalysts reported for the same reaction, and the results are listed in Table 3. In the present work, the catalyst with the hydrophobic group, $[Cr_3O(BDC–SO_3H)_{2.4}(BDC–SO_3NH_3Bu)_{0.6}]_n$ (20% $BuNH_2$), in addition to having a better catalytic performance than other reported catalysts, also has the advantage of decreasing reaction time and amount of catalyst, which makes the process economically beneficial.

3.3. Catalyst recycling

One of the major issues in the use of a catalyst is the recovery and recycling of catalysts. In this regard, the potential for recovery and recycling of the catalyst was evaluated. In this context, after

Table 2
Effect of hydrophobic group of catalyst on the esterification yields of phthalic anhydride with various alcohols in presence of $[Cr_3O(BDC–SO_3H)_{2.4}(BDC–SO_3NH_3–Bu)_{0.6}]_n$ (20% $BuNH_2$) (A) and MIL-101(Cr)–SO_3H (B).

Entry	Alcohol	Catalyst	Yield[a] (%)
1	CH_3CH_2OH	A	97.0
2	CH_3CH_2OH	B	70.0
3	CF_3CH_2OH[b]	A	60.2
4	CF_3CH_2OH	B	40.3
5	$CH_3CH_2CH_2CH_2OH$	A	98.0
6	$CH_3CH_2CH_2CH_2OH$	B	92.0
7	$CH_3CH_2CH_2CH_2CH_2CH_2OH$	A	72.5
8	$CH_3CH_2CH_2CH_2CH_2CH_2OH$	B	68.7

Reaction conditions: phthalic anhydride (4 mmol) and alcohol (20 mmol), catalyst (60 mg), reaction temperature: reflux, time: 5 h.

[a] Isolated yield.

[b] The ester prepared from alcohol in entry 3 is reported for the first time.

Table 3
Comparison of MIL-101(Cr)–SO_3H and $[Cr_3O(BDC–SO_3H)_{2.4}(BDC–SO_3NH_3Bu)_{0.6}]_n$ (20% $BuNH_2$) catalytic efficiency with other catalysts reported for esterification of phthalic anhydride with ethanol.

Entry	Catalyst	Amount of catalyst (g)	PhA/EtOH[a]	T (°C)	Time (h)	Yield (%)	Ref.
1	HFDAIL[b]	0.05	1:5	125	24	50	[37]
2	Sulfonated graphene	0.15	1:excess	120	3	93	[56]
3	A[c]	0.06	1:5	78	5	97	This work
4	B[d]	0.06	1:5	78	5	70	This work

[a] Mole ratio of phthalic anhydride to ethanol.
[b] Hydroxyl functionalized diacidic ionic liquid.
[c] $[Cr_3O(BDC–SO_3H)_{2.4}(BDC–SO_3NH_3Bu)_{0.6}]_n$ (20% $BuNH_2$) (A).
[d] MIL-101(Cr)–SO_3H (B).

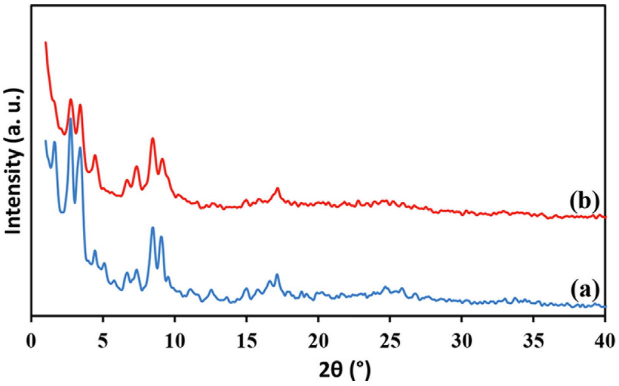

Fig. 8. Powder XRD patterns of the fresh $[Cr_3O(BDC–SO_3H)_{2.4}(BDC–SO_3NH_3Bu)_{0.6}]_n$ (20% $BuNH_2$) (a), and recycled $[Cr_3O(BDC–SO_3H)_{2.4}(BDC–SO_3NH_3Bu)_{0.6}]_n$ (20% $BuNH_2$) (b).

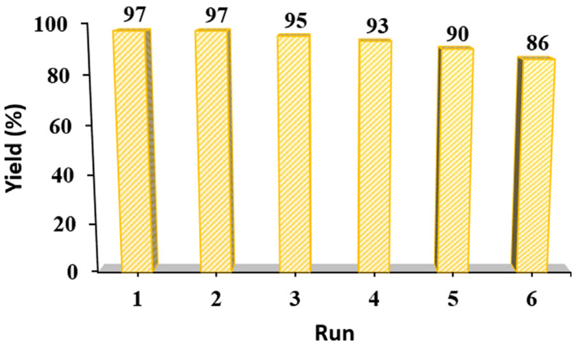

Fig. 9. Recycling of $[Cr_3O(BDC–SO_3H)_{2.4}(BDC–SO_3NH_3Bu)_{0.6}]_n$ (20% $BuNH_2$) in the synthesis of diethylphthalate.

completion of the reaction, the catalyst was separated by centrifugation, washed with dichloromethane, dried at 50 °C, and then used in the next reaction. The results showed that the recovered $[Cr_3O(BDC–SO_3H)_{2.4}(BDC–SO_3NH_3Bu)_{0.6}]_n$ (20% $BuNH_2$), while retaining its structures according to the XRD analysis (Fig. 8), could catalyze the esterification reaction in several consecutive runs without significant loss of activity (Fig. 9).

4. Conclusions

In summary, the incorporation of hydrophobic groups along with acidic groups in mesoporous MIL-101(Cr), has a synergistic effect on the esterification of phthalic anhydride with hydrophilic and acidic alcohols. It has been demonstrated that mesoporous MIL-101(Cr)–SO_3H and $[Cr_3O(BDC–SO_3H)_{2.4}(BDC–SO_3NH_3Bu)_{0.6}]_n$ (20% $BuNH_2$) could act as potent and robust catalysts in the esterification of phthalic anhydride. The effect of different parameters, including the type of alcohol, amount of catalyst, time, temperature, the mole ratio of reactants, and the hydrophobic moiety in solid acid on the reaction was investigated. Finally, it should be mentioned that $[Cr_3O(BDC–SO_3H)_{2.4}(BDC–SO_3NH_3Bu)_{0.6}]_n$ can be a valuable acid catalyst for increasing yields of other low-yield organic transformation reactions that need an acid catalyst and produce water as a side product.

Acknowledgment

The financial support (Grant number S600/43) from the Research Council of Shahid Beheshti University gratefully acknowledged.

Appendix A. Supplementary data

Supplementary data to this article can be found online at https://doi.org/10.1016/j.poly.2019.114142.

References

[1] O.M. Yaghi, M. O'keeffe, N.W. Ockwig, H.K. Chae, M. Eddaoudi, J. Kim, Nature 423 (2003) 705.
[2] N. Stock, S. Biswas, Chem. Rev. 112 (2011) 933.
[3] S. Kitagawa, R. Kitaura, S.I. Noro, Angew. Chem. Int. Ed. 43 (2004) 2334.
[4] M. Massoudinejad, M. Ghaderpoori, A. Shahsavani, M.M. Amini, J. Mol. Liq. 221 (2016) 279.
[5] M.P. Suh, H.J. Park, T.K. Prasad, D.-W. Lim, Chem. Rev. 112 (2011) 782.
[6] E. Gulcay, I. Erucar, Ind. Eng. Chem. Res. 58 (2019) 3225.
[7] I.A. Lázaro, R.S. Forgan, Coord. Chem. Rev. 380 (2019) 230.
[8] H. Hosseini, H. Ahmar, A. Dehghani, A. Bagheri, A.R. Fakhari, M.M. Amini, Electrochim. Acta 88 (2013) 301.
[9] A. Corma, H. García, F. Llabrés i Xamena, Chem. Rev. 110 (2010) 4606.
[10] R. Mohammadian, M.K. Alavijeh, N. Kamyar, M.M. Amini, A. Shaabani, Polyhedron 156 (2018) 174.
[11] M.B. Boroujeni, A. Hashemzadeh, M.-T. Faroughi, A. Shaabani, M.M. Amini, RSC Adv. 6 (2016) 100195.
[12] A. Shaabani, R. Mohammadian, H. Farhid, M.K. Alavijeh, M.M. Amini, Catal. Lett. 149 (2019) 1237.
[13] Z. Hasan, J.W. Jun, S.H. Jhung, Chem. Eng. J. 278 (2015) 265.
[14] J.C. Manayil, V.C. dos Santos, F.C. Jentoft, M. Granollers Mesa, A.F. Lee, K. Wilson, ChemCatChem 9 (2017) 2231.
[15] J.-P. Dacquin, H.E. Cross, D.R. Brown, T. Düren, J.J. Williams, A.F. Lee, K. Wilson, Green Chem. 12 (2010) 1383.
[16] J.G. Nguyen, S.M. Cohen, J. Am. Chem. Soc. 132 (2010) 4560.
[17] C. Yang, U. Kaipa, Q.Z. Mather, X. Wang, V. Nesterov, A.F. Venero, M.A. Omary, J. Am. Chem. Soc. 133 (2011) 18094.
[18] L. Ma, L. Xu, H. Jiang, X. Yuan, RSC Adv. 9 (2019) 5692.
[19] J. Lunagariya, A. Dhar, R.L. Vekariya, RSC Adv. 7 (2017) 5412.
[20] U. Widmer, Synthesis 1983 (1983) 135.
[21] B. Stanovnik, M. Tisler, A. Hribar, G. Barlin, D. Brown, Aust. J. Chem. 34 (1981) 1729.
[22] E. Mohacsi, Synth. Commun. 12 (1982) 453.
[23] W. Hao, T. Fujii, T. Dong, Y. Wakai, T. Yoshimura, Heteroatom Chem. 15 (2004) 193.
[24] J. Boivin, E. Henriet, S.Z. Zard, J. Am. Chem. Soc. 116 (1994) 9739.
[25] H. Meerwein, P. Borner, O. Fuchs, H.J. Sasse, H. Schrodt, J. Spille, Chem. Ber. 89 (1956) 2060.
[26] H. Meerwein, G. Hinz, P. Hofmann, E. Kroning, E. Pfeil, Adv. Synth. Catal. 147 (1937) 257.
[27] W.N. Haworth, J. Chem. Soc., Trans. 107 (1915) 8.
[28] F.H. Stodola, J. Org. Chem. 29 (1964) 2490.

[29] J. Grundy, B. James, G. Pattenden, Tetrahedron Lett. 13 (1972) 757.
[30] F. Ogura, H. Yamaguchi, T. Otsubo, T. Nakano, T. Saito, Bull. Chem. Soc. Jpn. 56 (1983) 1257.
[31] H.M. Bolt, B. Gansewendt, Crit. Rev. Toxicol. 23 (1993) 237.
[32] J. McCann, E. Choi, E. Yamasaki, B.N. Ames, Proc. Nat. Acad. Sci. 72 (1975) 5135.
[33] C. Zhang, G. Zhang, S. Luo, C. Wang, H. Li, Org. Biomol. Chem. 16 (2018) 8467.
[34] P. Dawar, M.B. Raju, R.A. Ramakrishna, Synth. Commun. 44 (2014) 836.
[35] S.H. Park, J.S. Park, T.W. Ko, Y.S. Park, J.W. Woo, Adv. Mat. Res., Trans. Technol. Publ. 634 (2013) 642.
[36] M. Yasunori, A. Masatomo, Jpn. Pat. JP, 278840 (2001).
[37] R. Fareghi-Alamdari, M.N. Niri, H. Hazarkhani, J. Mol. Liq. 227 (2017) 153.
[38] Y. Leng, J. Wang, D. Zhu, X. Ren, H. Ge, L. Shen, Angew. Chem. 121 (2009) 174.
[39] C. Xie, H. Li, L. Li, S. Yu, F. Liu, J Hazard Mater. 151 (2008) 847.
[40] H. Xing, T. Wang, Z. Zhou, Y. Dai, Ind. Eng. Chem. Res. 44 (2005) 4147.
[41] A.G. Khiratkar, K.R. Balinge, M. Krishnamurthy, K. Cheralathan, D.S. Patle, V. Singh, S. Arora, P.R. Bhagat, Catal. Lett. 148 (2018) 680.
[42] Z.I. Ishak, N.A. Sairi, Y. Alias, M.K.T. Aroua, R. Yusoff, Catal. Rev. 59 (2017) 44.
[43] N. Mansir, Y.H. Taufiq-Yap, U. Rashid, I.M. Lokman, Energy Convers. Manage. 141 (2017) 171.
[44] M. Arabi, M.M. Amini, M. Abedini, A. Nemati, M. Alizadeh, J. Mol. Catal. A: Chem. 200 (2003) 105.
[45] P.S. Kong, P. Cognet, Y. Pérès, J. Esvan, W.M.A.W. Daud, M.K. Aroua, Ind. Eng. Chem. Res. 57 (2018) 9386.
[46] P. Prinsen, R. Luque, C. González-Arellano, Microporous Mesoporous Mater. 262 (2018) 133.
[47] L.L. Rade, C.O. Lemos, M.A.S. Barrozo, R.M. Ribas, R.S. Monteiro, C.E. Hori, Renewable Energy 115 (2018) 208.
[48] L. Bromberg, Y. Diao, H. Wu, S.A. Speakman, T.A. Hatton, Chem. Mater. 24 (2012) 1664.
[49] G. Akiyama, R. Matsuda, H. Sato, M. Takata, S. Kitagawa, Chem. Mater. 23 (2011) 3294.
[50] A. Klinkebiel, N. Reimer, M. Lammert, N. Stock, U. Lüning, Chem. Commun. 50 (2014) 9306.
[51] M.G. Goesten, J. Juan-Alcañiz, E.V. Ramos-Fernandez, K.S.S. Gupta, E. Stavitski, H. van Bekkum, J. Gascon, F. Kapteijn, J. Catal. 281 (2011) 177.
[52] Y. Zang, J. Shi, F. Zhang, Y. Zhong, W. Zhu, Catal. Sci. Technol. 3 (2013) 2044.
[53] J. Chen, Z. Zhang, Z. Bao, Y. Su, H. Xing, Q. Yang, Q. Ren, ACS Appl. Mater. Interfaces 9 (2017) 9772.
[54] D. Zhang, F. Ye, Y. Guan, Y. Wang, E.J. Hensen, RSC Adv. 4 (2014) 39558.
[55] R. Thakkar, U. Chudasama, Green Chem. Lett. Rev. 2 (2009) 61.
[56] B. Garg, T. Bisht, Y.-C. Ling, RSC Adv. 4 (2014) 57297.